DOI: https://doi.org/10.68732/03e911ef7ba91e4b

ISBN: 978-9989-2053-6-1

Safe Footing Distance for an Isolated Footing Adjacent to an Excavation Wall in Jointed Rock Masses

Argha Biswas, Mahendra Singh & Aditya Singh
Department of Civil Engineering, IIT Roorkee, Uttarakhand, India
arghab73@gmail.com
0009-0008-1375-5679

Abstract

Increasing land-use pressure often requires engineers to construct structures in close proximity to a vertical cut and supported by a retaining wall, particularly in hilly regions. In such cases, the distance of a footing from the vertical cut or excavation becomes a critical parameter, as it governs the extent to which excavation-induced effects can be minimized or neglected. Although footings may be placed on either soil or rock, identifying a safe footing location on jointed rock is considerably more complex due to the anisotropic behavior of jointed rock masses compared with the relatively isotropic nature of soils. To investigate this, 2D physical model tests were conducted on an artificial 60°–30° orthogonally jointed rock mass with an isolated footing placed adjacent to an excavation wall. The experimental results indicate that when the footing is positioned beyond a certain safe footing distance, the excavation no longer affects the bearing capacity, regardless of the excavation depth. Complementary finite element modeling analysis was conducted to assess the bending-moment distribution, shear-stress distribution, and load transfer along the excavation wall. The numerical results likewise demonstrate that beyond the safe footing distance, bending moments and shear stresses applied exhibit similar patterns for different excavation depths.

Keywords

Excavation wall, Artificial rock mass, Physical model, Safe footing distance, Finite element modelling.

1 Introduction

Population growth and rapid urbanisation have intensified land-use pressure, particularly in mountainous terrains. This often necessitates the construction of critical infrastructure in geologically unfavourable locations, such as in close proximity to vertical rock cuts or excavations. In such projects, retaining structures are frequently employed to provide lateral support. However, the offset distance between the footing and the excavation face constitutes a critical design parameter, as it controls the extent to which excavation-induced stress redistribution affects the foundation.

Numerous studies have investigated the behaviour of foundations located near vertical cuts in soils. However, the direct applicability of these findings to foundations placed adjacent to vertical excavations in jointed rock masses is limited due to the presence of discontinuities. Because of the isotropic properties of soil, the stress distribution beneath an applied load follows a symmetrical circular pattern. In contrast, the presence of joints imparts anisotropy to rock masses, resulting in a non-uniform, direction-dependent stress distribution that deviates from the conventional circular symmetry (Boussinesq, 1885; Goodman, 1991, Biswas et al 2025b).

A limited number of studies have investigated foundations located near vertical cuts in jointed rock masses. Biswas et al. (2025a, 2025b) performed physical model studies on orthogonally jointed rock masses with a foundation placed adjacent to an excavation wall. Previously, Son and Park (2014) employed both physical model tests and numerical simulations to investigate the earth pressure acting on excavation walls in single-jointed rock at varying excavation depths. Subsequently, Son and Adedokun conducted a series of numerical parametric studies to evaluate earth pressure distributions under diverse conditions, including joint cohesion (2014), layered jointed rock masses (2016), joint inclination (2017a), rock mass quality, ranging from hard to highly weathered (2017b, and wall permeability (2018). However, in these studies by Son and Park (2014) and Son and Adedokun (2014, 2016, 2017a, 2017b, 2018), the foundation was not placed on the jointed rock mass; consequently, the effect of footing distance from the excavation was not examined.

To investigate this, 2D physical model tests were conducted on an artificial 60°–30° orthogonally jointed rock mass with an isolated footing placed adjacent to an excavation wall. Complementary finite element modelling (FEM) was conducted to assess the bending moment distribution, shear stress distribution, and load transfer along the excavation wall for different footing distances.

2 Physical model tests

A series of 2D physical model tests, scaled at 1:20, were performed in the Geotechnical Engineering laboratory at IIT Roorkee to examine the bearing capacity and load-settlement characteristics of isolated footings with varying footing positions and excavation depth. This model rock mass comprised two continuous orthogonal joint sets: one dipping at 60° toward the excavation and the other orthogonal to it, oriented at 30°.

The artificial rock mass was formed using individual blocks (25 mm × 25 mm × 75 mm) cast from a blend of Plaster of Paris, white cement, sand, and water. These blocks were meticulously assembled into a 1.2 m × 0.8 m × 0.15 m configuration to represent the 60°–30° orthogonal joint sets. To represent the excavation boundary, a 0.4 m high acrylic sheet (10 mm thick) was utilised.

As shown in the Fig 1, a rigid foundation was simulated using a 0.15 m square mild steel plate (0.025 m thick) placed on the artificial rock mass upper surface. Vertical loading was applied via a 300 kN capacity hydraulic jack and monitored through a 350 kN proving ring. Foundation settlement was recorded using two dial gauges positioned at the midpoints of opposite edges of the plate. The mechanical properties of the constituent materials and joint interfaces, determined through a comprehensive testing suite (including UCS, triaxial, Brazilian, and direct shear tests), are summarised in Table 1. Further experimental details are documented in Biswas et al. (2025b).

Physical model tests were performed with the footing located at offset distances of 0B, 1B, and 2B from the excavation face, where B is the footing width, 0.15 m. The minimum embedment depth of 0.25h (h representing the wall height) was maintained throughout the experimental program.

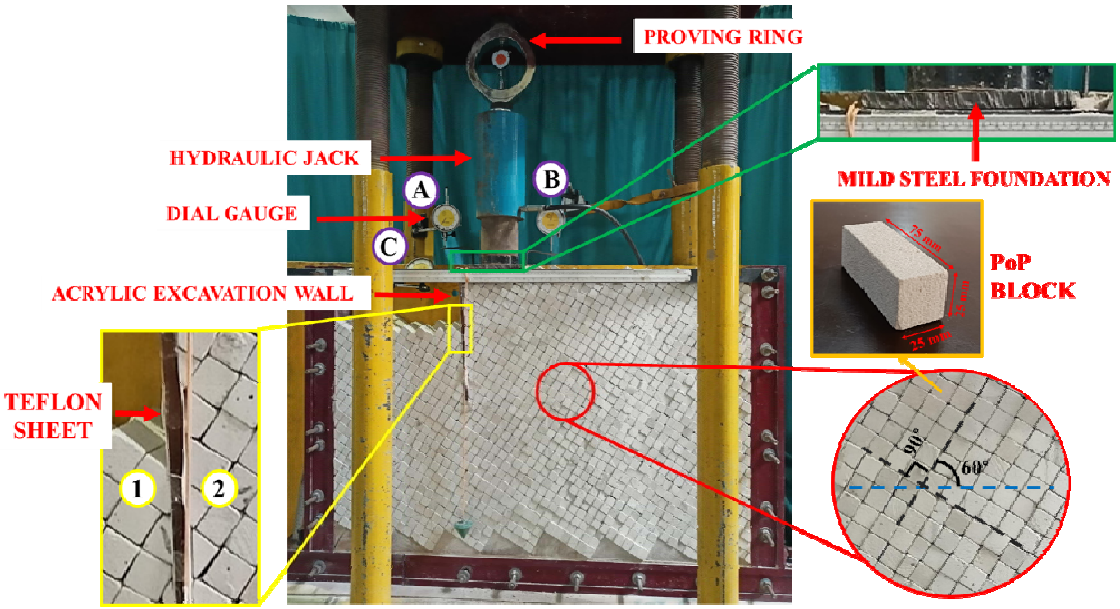


Fig. 1 Experimental setup at the Geotechnical Engineering Laboratory, IIT Roorkee (Biswas et al., 2025b).

Table 1. Material and interface properties.

Material properties		
	Artificial rock	**Excavation wall**
Constitutive model	**Mohr-coulomb plastic**	**Linear elastic**
E (MPa)	2450	3040
γ (kN/m^3)	16.37	11.5
ν	0.3	0.37
c (MPa)	3.2	26
ϕ (°)	31.2	0
Interface properties		
	Rock joint	**Wall and Rock**
Constitutive model	**Coulomb slip**	**Coulomb slip**
K_n(MPa/m)	700	150
K_s (MPa/m)	70	15
c (kPa)	8	0
ϕ (°)	37.6	0

3 Physical model tests results

Figure 2 shows the footing pressure versus vertical settlement of the 60°–30° jointed rock mass for different excavation depths and footing positions. Figure 2(a) shows that for the 0B footing location, the failure stress or bearing capacity decreases rapidly as the excavation depth increases; at a high excavation depth (0.3 m), the rock mass failed under its own weight, so no settlement curve is obtained. Figure 2(b) shows that for the 1B footing, the bearing capacity decreases with increasing excavation depth, but the rate of decrease is less than that of the 0B position. Figure 2(c) shows that for the 2B footing, there is no decrease in the bearing capacity as the excavation height increases. This figure demonstrates that as the footing distance from the excavation wall increases, the excavation effect on the foundation becomes negligible or zero.

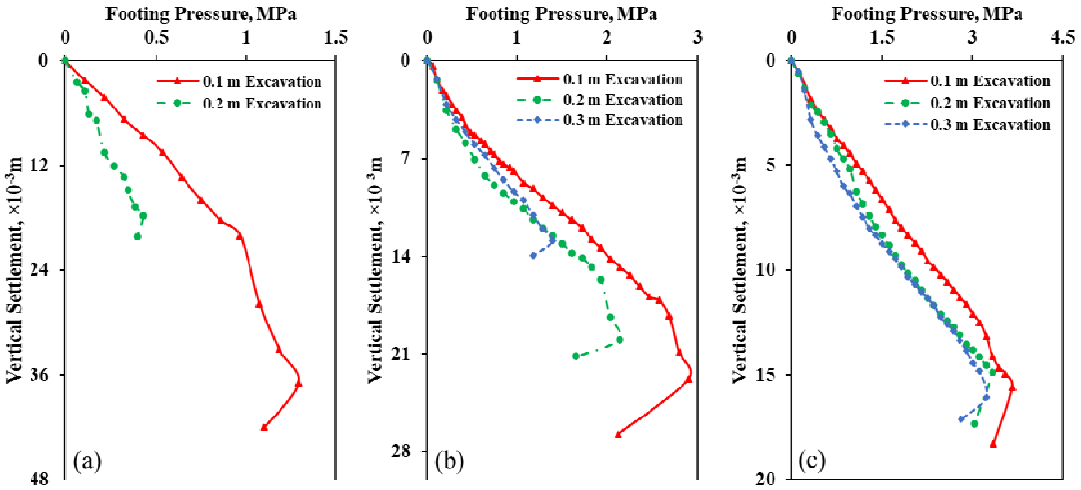


Fig. 2 Footing pressure vs vertical settlement curve for varying excavation depths and footing positions.

4 Numerical modeling and results

In this study a Finite element modelling was created using the Rocscience software (RS2, version 11.026). The numerical model was developed based on the measured physical properties listed in Table 1. To simulate the behavior of the intact rock, Mohr-Coulomb plastic constitutive model was employed, while the flexible excavation wall was modeled using linear elastic properties. Additionally, the Coulomb slip constitutive model was used to simulate the mechanical behavior of the rock joints.

Figures 4 and 5 show the numerical modelling results. Figure 4 shows the bending moment distribution along the excavation wall for different footing positions and excavation depths. In Figures 4(a) and 4(b), when the footing is placed at 0B and 1B distances from the excavation wall, the bending moment distribution varies significantly with the excavation depth. However, when the footing is positioned at a 2B distance, the bending moment distribution exhibits a similar pattern across all depths, as shown in Figure 4(c). For the footing positioned at 2B, the 0.3 m excavation depth results in greater lateral movement of the excavation wall compared to the 0.1 m and 0.2 m depths. Consequently, as shown in Fig. 4(c), while the overall profile of the bending moment distribution remains consistent, the magnitudes are lower than those recorded for the shallower excavation depths.

Figure 5 shows the applied stress distribution along the excavation wall, which exhibits a similar tendency to the bending moment distribution. When the footing is placed at the 0B and 1B positions, the applied stress distribution changes rapidly with variations in excavation depth. However, for the 2B footing distance, the stress distribution shows similar trends and consistent values across all excavation depths.

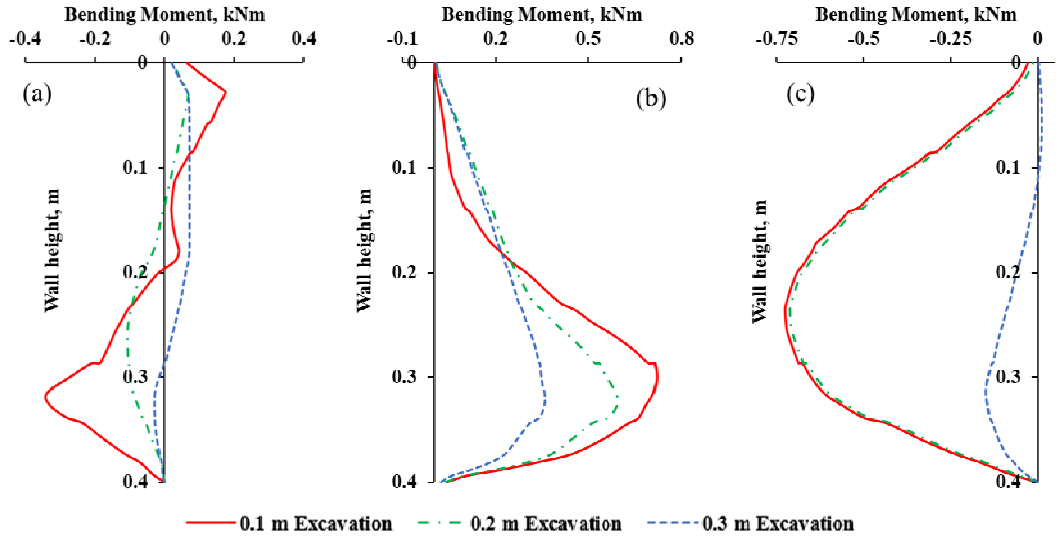


Fig. 3 Bending moment distribution along the excavation wall.

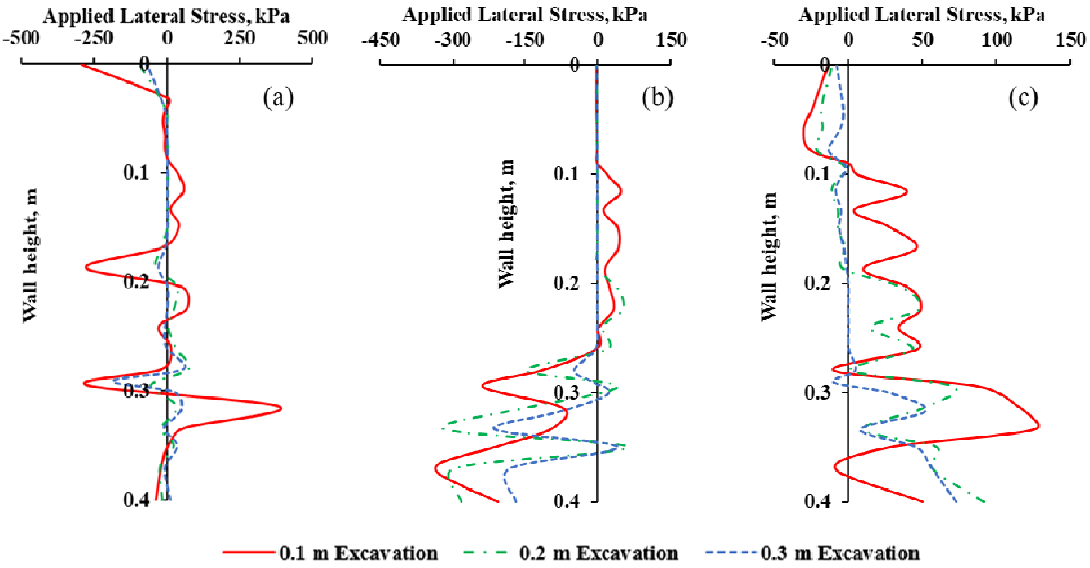


Fig. 4 Applied lateral stress distribution along the excavation wall.

Based on these results, it can be concluded that when a footing is positioned beyond a certain horizontal distance from the excavation wall, the excavation depth no longer influences foundation performance. Beyond this critical distance, the stress distribution generated by the footing does not intersect with the excavation face; instead, the load is fully contained within the rock mass, allowing the system to behave as an unexcavated rock mass (Fig. 5). In the present study, this threshold is defined as the "safe footing distance". For an embedment depth of at least 0.25h, this distance is mathematically expressed as h·cot(θ), where h denotes the height of the excavation wall and θ represents the inclination of the joint set dipping toward the wall (measured from the horizontal).

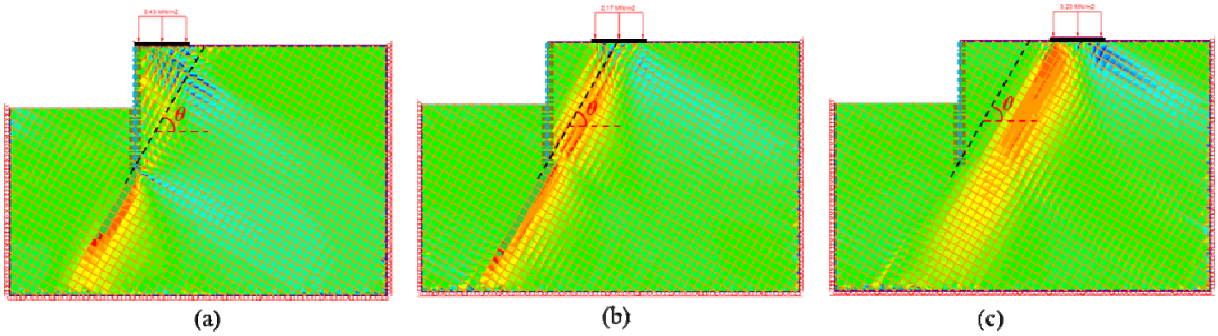


Fig. 5 Total stress distribution for the 60°–30° orthogonally jointed rock mass with an excavation depth of 0.2 m for footing positioned at (a) 0B, (b) 1B, and (c) 2B. The black dashed line indicates the h·cot (θ) horizontal distance for this rock mass (Biswas et al., 2026).

5 Conclusions

Experimental results indicate that for footings located in close proximity to a vertical cut (0B and 1B), the bearing capacity is significantly influenced by excavation depth. In contrast, at a footing offset distance of 2B, the bearing capacity remains nearly constant across all excavation depths, suggesting a negligible influence of excavation depth on the foundation. Finite element analyses further corroborate these findings, showing that at a 2B distance, both the bending moment and stress distribution along the excavation wall exhibit similar patterns regardless of excavation depth, unlike the variations observed for 0B and 1B conditions.

This behaviour can be attributed to the fact that the stress distribution induced by the footing does not intersect the excavation face at this distance; instead, it remains confined within the rock mass, allowing the system to behave comparably to an unexcavated condition. The identified threshold distance, beyond which excavation-induced effects become negligible, is defined as the safe footing distance.

References

Biswas A, Singh A, Singh M (2025) Experimental investigation and a method of calculating bearing capacity for jointed rock masses under excavated and unexcavated conditions. Rock Mechanics and Rock Engineering.

Biswas A, Singh A, Singh M (2025) The effects of staggered and non-staggered joints on the ultimate bearing capacity, load settlement behavior, and failure mechanism with the change of excavation depths. Rock Mechanics Bulletin 4(1): 100154.

Biswas A, Singh A, Singh M (2025) Comprehensive analysis of excavation walls in jointed rock masses: bending moment, applied stress distribution, and empirical load estimation. (Submitted).

Son M, Adedokun S (2014) Effect of joint cohesive strength on the earth pressure against the support system in a jointed rock mass. Journal of the Korean Geotechnical Society 30(7): 41–53.

Son M, Adedokun S (2015) Effect of support characteristics on the earth pressure in a jointed rock mass. Canadian Geotechnical Journal 52(12): 1956–1967.

Son M, Adedokun S (2016) Effect of joint inclination angles on the earth pressure against the support system in a jointed rock mass. KSCE Journal of Civil Engineering 20(4): 1259–1266.

Son M, Adedokun S (2017a) Earth pressure on a retaining structure in layered and jointed rock masses. KSCE Journal of Civil Engineering 21(4): 1147–1153.

Son M, Adedokun S (2017b) Effect of rock mass condition on the earth pressure against an excavation wall in rock mass: numerical investigation. Journal of the Korean Geotechnical Society 33(11): 83–95.

Son M, Adedokun S (2018) Effect of the permeability of excavation wall on the earth pressure in a jointed rock mass. KSCE Journal of Civil Engineering 19(2): 13–21.

Son M, Park J (2014) Physical and numerical tests of the excavation walls in jointed rock masses. Canadian Geotechnical Journal 51(5): 554–569.